ev, M., Mohseni, E., Vithanage, R. K. W., MacLeod, C. N., Pierce, G., Mehnen, J., & Gachagan, A. (2022). Development of a phased array ultrasonic system for residual s

**Proceedings of the ASME 2022
Pressure Vessels & Piping Conference
PVP2022
July 17 - 22, 2022, Las Vegas, Nevada, USA**

PVP2022-85023

DEVELOPMENT OF A PHASED ARRAY ULTRASONIC SYSTEM FOR RESIDUAL STRESS MEASUREMENT IN WELDING AND ADDITIVE MANUFACTURING

Yashar Javadi[1,2,*], Alistair Hutchison[1], Rastislav Zimermann[1], David Lines[1], Nina E. Sweeney[1], Momchil Vasilev[1], Ehsan Mohseni[1], Randika K.W. Vithanage[1], Charles N. MacLeod[1], Gareth Pierce[1], Jorn Mehnen[2], and Anthony Gachagan[1]

[1] Centre for Ultrasonic Engineering (CUE), Department of Electronic & Electrical Engineering (EEE), University of Strathclyde, Glasgow G1 1XQ, UK
[2] Department of Design, Manufacturing & Engineering Management (DMEM), University of Strathclyde, Glasgow G1 1XQ, UK

ABSTRACT

Residual Stress (RS) in engineering components can lead to unexpected and dangerous structural failures, and thus represent a significant challenge to quality assurance in both welding and metal additive manufacturing (AM) processes. The RS measurement using the ultrasonic method is based on the acoustoelasticity law, which states that the Time-of-Flight (ToF) of an ultrasonic wave is affected by the stress field. Longitudinal Critically Refracted (LCR) waves have the highest sensitivity to the stress in comparison with the other type of ultrasonic waves. However, they are also sensitive to the material texture which negatively affects the accuracy of the RS measurement. In this paper, a Phased Array Ultrasonic Testing (PAUT) system, rather than the single element transducers which are traditionally used in the LCR stress measurement technique, is innovatively used to enhance the accuracy of RS measurement. An experimental setup is developed that uses the PAUT to measure the ToFs in the weld, where the maximum amount of tensile RS is expected, and in the parent material, stress-free part. The ToF variations are then interpreted and analyzed to qualify the RS in the weld. The same measurement process is repeated for the Wire Arc Additive Manufacture (WAAM) components. Based on the results, some variations between different acoustic paths are measured which prove that the effect of the residual stress on the ultrasonic wave is detectable using the PAUT system.

Keywords: Residual Stress (RS); Phased Array Ultrasonic Testing (PAUT); Wire Arc Additive Manufacture (WAAM); Longitudinal Critically Refracted (LCR) Waves.

1. INTRODUCTION

The residual stress produced in a variety of manufacturing processes, from welding [1] and additive manufacturing [2] to forming [3] and machining [4], can lead to catastrophic failure in components made from a wide range of materials, from Cr-Mo F22 forging steel [5] used in the Oil and Gas industry to nuclear grade P91 steel [6] and titanium [2] or composite structures [7] used in aerospace. Both welding and Wire Arc Additive Manufacture (WAAM) transfer a large amount of heat energy into a small area in a short time, which leads to the development of significant distortion and residual stresses [2]. The residual stress, remaining inside the material in the absence of any external loads or thermal gradients, can lead to unexpected structural failure on a large scale with very serious consequences. For example, the residual stress was believed to be one of the major factors encouraging the growth of a small crack in a cast eyebar link causing the loss of 46 lives during the failure of the Silver Bridge in West Virginia in 1967 [8]. Even in 2021, residual stress is still a major issue in industry and particularly in welding and WAAM. For example, Javadi et al [9] showed that an increase of 78 MPa in welding residual stress can result in a considerable increase in length and width of a hydrogen induced crack; i.e., a 13 mm crack was detected in the high residual stress sample while the crack length was <2 mm in the low residual stress sample (see Figure 1). It should be noted that the material Yield Strength was 480 MPa and the excessive amount of weld residual stress (78 MPa) had been produced by a small modification in the position of the clamps. This is even more concerning in WAAM in which a near-yield tensile residual stress for aluminium and Inconel (around 1000 MPa) was reported in another 2021 paper [10].

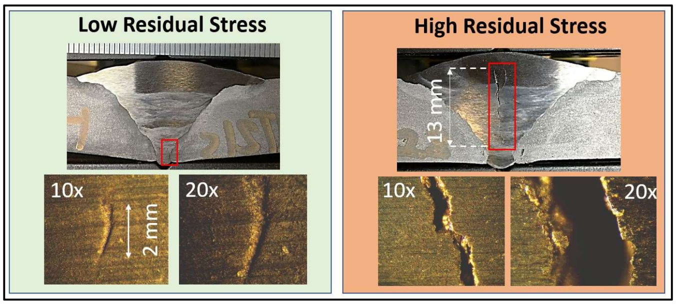

FIGURE 1: THE EFFECT OF RESIDUAL STRESS ON THE HYDROGEN-INDUCED CRACK IN THE WELD [1]

Therefore, the measurement and mitigation of the residual stress is an essential procedure, especially in safety-critical components [11]. The measurement of welding and WAAM residual stresses can be achieved through non-destructive methods (e.g., ultrasonic techniques [12]), semi-destructive methods (e.g., hole-drilling [13], which is the only standardised method by ASTM E837) or destructive methods (e.g., the contour method [14]).

In this paper, the ultrasonic method is investigated for the residual stress measurement in the weld and WAAM components. The main benefits of using the ultrasonic method compared with the other Non-Destructive Evaluation (NDE) methods (neutron diffraction [15] and X-ray diffraction [16]) are as follows:

1) 3D distribution of the residual stress: The residual stress of hundreds of points can be measured using the ultrasonic method allowing a 3D evaluation of the residual stress [12].
2) Repeatability: The neutron diffraction technique is usually carried out in specialized facilities which typically require the submission of a measurement proposal, which can have significant processing time. This limits the possibility of repeating the measurement, in case the results are not acceptable after processing the data. On the other hand, the ultrasonic method will provide results that can be quickly processed during the welding/WAAM process and is easily repeatable, especially in a robotic system.
3) Accessibility: The ultrasonic equipment is more accessible than neutron and X-ray diffraction methods. For example, the neutron diffraction reported by Javadi et al [6] was carried out by the pulsed diffractometer ENGIN-X, at the ISIS facility, Rutherford Appleton Laboratory in Oxford, which is the only neutron diffraction facility in the UK (among 12 facilities in Europe).
4) Penetration depth: X-ray diffraction is considered as a surface stress measurement method [6] because its penetration depth is in the range of a few microns while the ultrasonic method can simply measure the stresses in the depth of a few millimetres [12].

The main disadvantage of the ultrasonic method is the challenge of differentiating the material texture from the residual stress as both influences the ultrasonic wave. Furthermore, only the average of the residual stress is measurable using the ultrasonic method which can reduce the method selectivity in comparison with the other residual stress measurement techniques [17].

2. THEORETICAL BACKGROUND

2.1 RS Measurement using the ultrasonic method (traditional method)

The ultrasonic method for residual stress measurement works based on the acoustoelasticity law, which states that the material stress can affect the Time-of-Flight (ToF) of the ultrasonic wave. Egle and Bray [18] showed that the Longitudinal Critically Refracted (LCR) waves have a higher sensitivity to stress in comparison with other types of ultrasonic waves. The ToF of the longitudinal waves, parallel to the stress direction, can be related to the strain (α) through the following equation:

$$\rho_1 {V_{11}}^2 = \lambda + 2\mu + (2l + \lambda)\theta + (4m + 4\lambda + 10\mu)\alpha_1 \qquad (1)$$

where ρ_1 is the density; V_{11} is the wave velocity of the longitudinal wave (parallel to load); λ and μ are the second-order elastic constants (Lame's constants) and l and m are the third-order elastic constants. In Equation (1), $\theta=\alpha_1+\alpha_2+\alpha_3$ where α_1, α_2 and α_3 are components of the homogeneous triaxial principal strains. With the assumption of uniaxial stress, α_1 is equal to ε and both α_2 and α_3 are equal to $-\nu\times\varepsilon$, where ε is the strain in the direction 1 (parallel to the stress) and ν is the Poisson's ratio. Using these values, Equation (1) becomes:

$$\rho_1 {V_{11}}^2 = \lambda + 2\mu + [4(\lambda + 2\mu) + 2(\mu + 2m) + \nu\mu(1 + \frac{2\lambda}{\mu})].\varepsilon \qquad (2)$$

The variation of the velocity with the strain, called relative sensitivity, is calculated by Equation (3).

$$\frac{dV_{11}/V_{11}}{d\varepsilon} = 2 + \frac{(\mu+2m)+\nu\mu(1+2l/\lambda)}{\lambda+2\mu} = L_{11} \qquad (3)$$

where L_{11} is the acoustoelastic constant. Equation (3) is rearranged to calculate the stress variation in terms of ToF variations (dt/t_1), as shown in Equation (4):

$$d\sigma = \frac{E(dV_{11}/V_{11})}{L_{11}} = \frac{E}{L_{11}}(dt/t_1) \qquad (4)$$

where $d\sigma$ is the stress variation, E is the elastic modulus and t_1 is the ultrasonic wave ToF in the stress-free material. The ultrasonic stress measurement is then based on the difference between the ultrasonic wave ToF in the stress-free material (T1) and material with the applied or residual stress (T2) as shown in Figure 2a and Equation (5):

$$\sigma = \frac{E}{L}\frac{(T2-T1)}{T1} \qquad (5)$$

It should be noted that the L_{11} in Equation (3) is related to V_{11}, the velocity of the longitudinal wave which is propagated parallel to the stress. Therefore, with the assumption of measuring the longitudinal residual stress using the longitudinal ultrasonic wave (see Figure 2c), the L_{11} is simplified as L in Equation (5). It is also possible to penetrate various thicknesses of the material using different ultrasonic frequencies (Figure 2b) to measure the through-thickness residual stress [12]. The ultrasonic transducers, transmitters and receivers are placed in a specially-designed wedge which can be moved freely over the component to extend the measurement coverage throughout the component (see Test Section in Figure 2c). By increasing the number of Test Sections, it will be possible to generate a 3D presentation of the stress in the X-Z plane for a specific depth (Y), as shown in Figure 2d, which can also be extended to different thicknesses using the various testing frequencies. The acoustoelastic coefficient (L in Equation 5) is a material property that is required to be measured during a controlled loading/unloading procedure, such as the standard tensile test [12]. The stress-relieved sample extracted from the weld, Heat Affected Zone (HAZ) and parent material are machined based on the requirements of the standard tensile test samples and then the same ultrasonic measurement system is installed during the tensile test procedure. However, the acoustoelastic coefficient can vary considerably in the weld, HAZ and parent material. Therefore, it is required to extract the tensile test specimen from the parent material and weld separately, and also reproduce the HAZ microstructure in a specimen extracted from the parent material based on the experimental procedure described by Javadi et al [12]. They extracted twelve specimens from the parent material and applied various thermal cycles (heating and cooling) to simulate the HAZ thermal cycle. The samples were then micro-etched to compare their microstructure and grain size with the HAZ grain size. The thermal cycle producing the microstructure similar to the HAZ was then selected to be applied on a new tensile test specimen. Therefore, the acoustoelastic coefficient was also measured on the HAZ sample. Because the acoustoelastic constant can even vary in the weld, particularly in dissimilar material welds [19], it is recommended to use a similar approach to reproduce different weld microstructures in various tensile test specimens allowing a comprehensive measurement of the acoustoelastic coefficient. An important challenge of the ultrasonic stress measurement method is the problem of average data measurement, i.e. an average of the residual stress in the area affected by the wave travel path is measured rather than point-based measurement [12, 19]. For example, the residual stress measured by 1 MHz transducers in 6 mm depth, see Figure 2b, can include both surface and bulk stress data. If the tensile stresses are developed in the surface while compressive stresses are in the bulk, there is a risk of measurement of zero stress by this transducer [19].

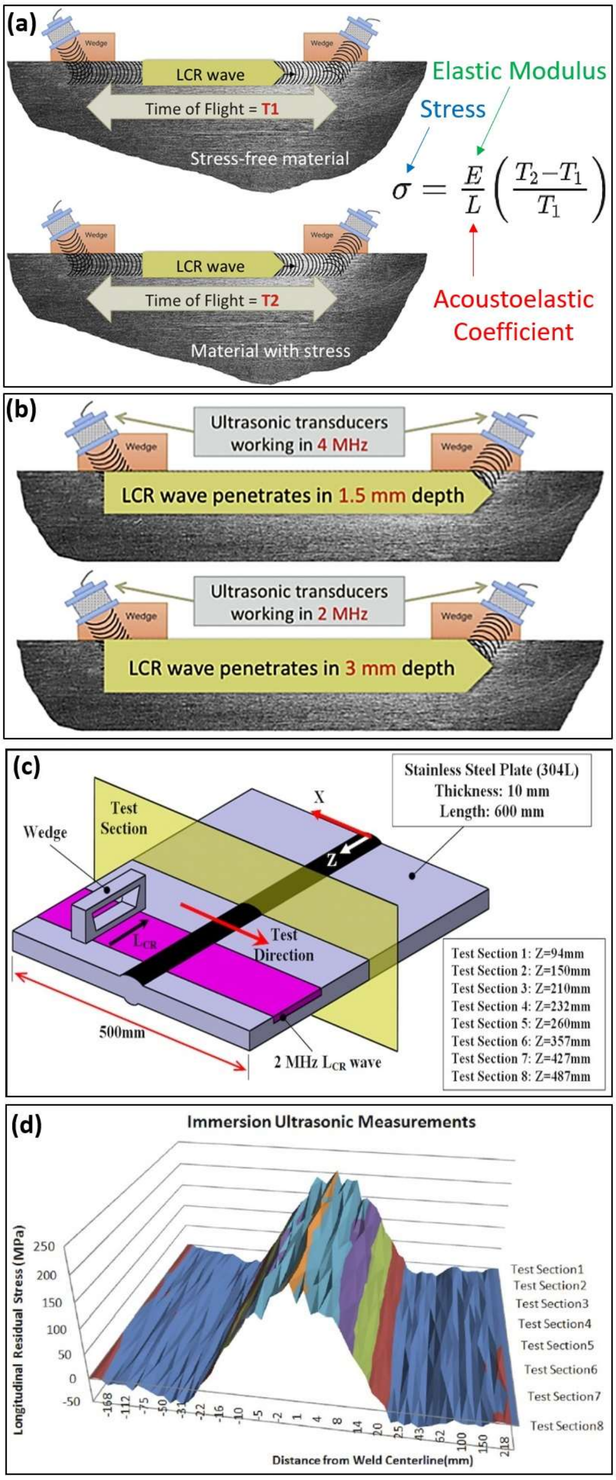

FIGURE 2: (A) THE MAIN CONCEPT OF THE ULTRASONIC STRESS MEASUREMENT [19], (B) THE POSSIBILITY OF THROUGH-THICKNESS STRESS MEASUREMENT [19], (C) THE CAPABILITY OF GENERATING VARIOUS TEST SECTIONS TO COVER THE WHOLE COMPONENT [20] AND (D) AN EXAMPLE OF A 3D DIAGRAM FOR THE RESIDUAL STRESS MEASUREMENT [20]

There are some techniques to deal with the averaging problem such as the FELCR method (combination of finite element welding simulation and LCR stress measurement) introduced by Javadi et al [12], increasing the number of measurement frequencies [21] and the application of both contact and immersion ultrasonic methods [20]. The severity of this problem can be reduced if the ultrasonic probe is small (therefore covering a small area of measurement) and if the distance of the wave propagation (acoustic path) is reduced.

The ultrasonic wave is sensitive to the material texture and microstructure which can reduce the accuracy of the residual stress measurement using the ultrasonic method [22]. This is improved by utilising the ultrasonic system during the tensile test method in which the same sample (with the same material texture) is stress-relieved. The measured stress value at the start of the test post-stress relieving (σ=0 MPa) represents T1.

2.2 RS Measurement using the ultrasonic method (PAUT method)

In this paper, the Phased Array Ultrasonic Testing (PAUT) system is used for the ultrasonic residual stress measurement rather than the single element transducers traditionally used for this purpose, as shown in Figure 3. Traditionally, it is recommended to use two receivers for the ultrasonic LCR stress measurement (see Figure 3a) in order to reduce the undesired effect of material texture and microstructure [12]. This is because the setup can generate two LCR wave paths (LCR Path 1&2 in Figure 3a), allowing for the effect of the residual stress on the ultrasonic ToF to be measured twice which can increase the measurement accuracy and reduce the material effects. If two arrays are used rather than the single element transducers, there will be many more LCR paths. For example, two 10 MHz arrays (16 elements) are shown in Figure 3b in an initial setup similar to the traditional LCR setup. The transmitter array can generate 16 ultrasonic waves (T1-T16) as it has 16 elements. Each of these 16 waves can be received by any of the 16 elements of the receiver array (R1 -R16). Therefore, a matrix of 16x16 LCR Paths can potentially be generated. As each of these 256 LCR Paths is different from the others (different distance or different position of the travel path in the material), 256 ToFs can be generated. This can potentially increase the measurement accuracy in comparison with the traditional setup which has only two LCR Paths.

The ultrasonic method is usually criticised in the application of residual stress measurement because the average residual stress is measured between the two receivers (in the traditional LCR setup) [19]. The distance between two receivers depends on the experimental setup and it was, for example, 34 mm in the setup developed by Javadi et al [19]. Therefore, any residual stress variation in this 34 mm distance is not measurable due to the averaging issue. However, this distance is dramatically reduced by using the PAUT system, as the distance is reduced to the array pitch(0.25-0.5 mm for Imasonic arrays used in this paper). The measurement resolution of 0.25 mm is very competitive and can bring the ultrasonic method to the top of the list of five major residual stress measurement considered in the round robin paper by Javadi et al [6], e.g., the hole-drilling (which is the only standard residual stress method) had a 2 mm diameter hole.

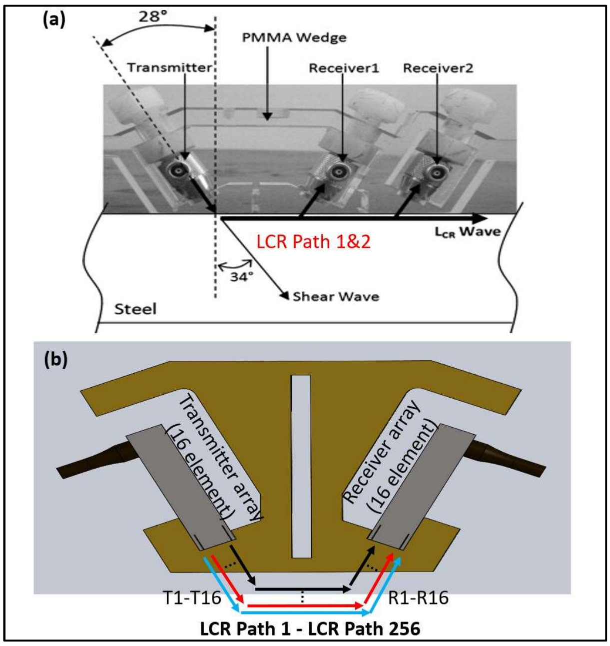

FIGURE 3: (A) TRADITIONAL ULTRASONIC LCR STRESS MEASUREMENT [12] AND (B) PAUT-LCR STRESS MEASUREMENT APPROACH PROPOSED IN THIS PROJECT

3. EXPERIMENTAL SETUP

3.1 Longitudinal ultrasonic wave (weld sample)

The first experiments included a metal strip (400 x 28.7 x 15 mm) cut from a larger weld plate (400 x 300 x 15 mm) as shown in Figure 4. The material was stainless steel (316L) with a thickness of 15 mm. The weld plate was manufactured using a Tungsten Inert Gas (TIG) welding process and a 304L electrode (ø1.2 mm). The process was fully automated and the sample was tested using the PAUT defect detection system to ensure there were no welding defects in the sample. After cutting the strip, the weld cap and root were ground to facilitate the ultrasonic inspection. This is known to be a drawback in ultrasonic residual stress measurement, as the welding cap is required to be left intact in the majority of welding applications [23]. However, if the PAUT system is developed for residual stress measurement, linking the system and in-process inspection during welding has been established by Javadi et al [9]. This paper recommended several experimental approaches, including using high-temperature rubber between the wedge and the weld cap to eliminate the requirement of removing the weld cap. Although outwith the scope of this paper, it is believed that the PAUT system has the potential to be used for in-process residual stress measurement.

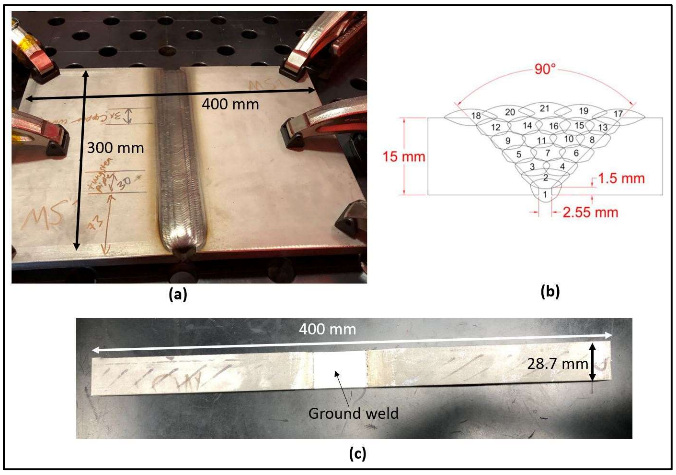

FIGURE 4: (A) WELD SAMPLE, (B) LAYOUT OF THE WELD PASSES AND (C) METAL STRIP (SPECIMEN)

Two ultrasonic arrays manufactured by Imasonic (France) were used to measure the ToF in different positions of the metal strip (parent material, HAZ and weld) as shown in Figure 5. The arrays were 5 MHz probes with 8 elements and a pitch of 0.5 mm. They are called Small Footprint Arrays as they are one of the smallest arrays commercially available (6 x 6.5 mm). Their small size is critical because the ultrasonic method is measuring the average of the residual stress in the area covered by the acoustic wave and the smaller probe area can increase the resolution of the measurement. The phased array controller used was FIToolbox (Diagnostic Sonar, UK) [24].

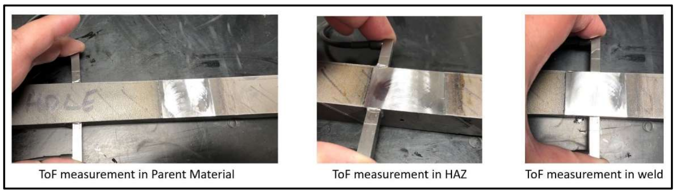
ToF measurement in Parent Material
ToF measurement in HAZ
ToF measurement in weld

FIGURE 5: ULTRASONIC TOF MEASUREMENT USING THE PAUT METHOD

3.2 Longitudinal ultrasonic wave (WAAM sample)

The second experiment included an aluminium WAAM sample as shown in Figure 6. The sample was manufactured by a robotic WAAM machine in a single bead deposition layout (as-built sample shown in Figure 5a) with 20 layers and 300 mm length. It was later machined to facilitate ultrasonic inspection (Figure 5b). The ultrasonic setup (Figure 5c) was the same as the setup used for the weld sample (Sec. 3.1)

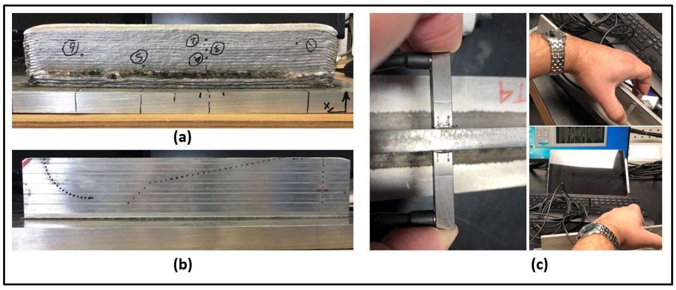

FIGURE 6: (A) AS-BUILT WAAM SAMPLE, (B) MACHINED WAAM SAMPLE AND (C) ULTRASONIC TOF MEASUREMENT USING THE PAUT METHOD ON THE MACHINED WAAM SAMPLE

3.3 PAUT-LCR wave

Although the longitudinal (normal) ultrasonic wave is suitable for WAAM inspection (Sec. 3.2), its application in weld sample testing is not as practical as with the WAAM sample. This is because the process currently cannot be implemented non-destructively and requires a weld strip to be removed by machining (Sec. 3.1). Therefore, a PAUT-LCR system was developed in this work to investigate the feasibility of conducting residual stress measurement on a weld sample (Figure 7).

FIGURE 7: PAUT-LCR SETUP ON THE WELD SAMPLE

4. RESULTS AND DISCUSSION

4.1 ToF variations in weld and WAAM

The ultrasonic arrays consist of 8 elements, allowing for the generation of a matrix of 8x8 ToFs recorded by two arrays in all three experiments (Figure 8). There must be a fixed point on the ultrasonic wave which is measured each time and compared with the other measurements. This point was chosen to be the 2nd Zero Crossing as shown in Figure 8. Therefore, a matrix of 64 ToFs, which represent the 2nd zero crossing, is extracted from each point of measurement using a MATLAB script linked to the LabView interface of the phased array controller.

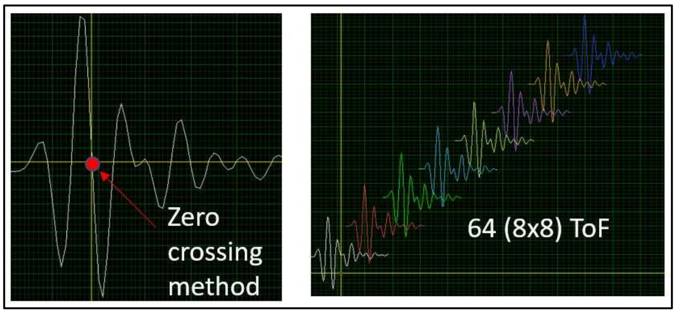

FIGURE 8: TOF MATRIX AND ZERO CROSSING APPROACH

The results include three separate matrices of 64 ToFs in parent material, HAZ and weld as listed in Table 1-3. All data is ToF (in microseconds) captured on the weld strip sample (Sec. 3.1). T1-8 represent the 8 elements of the transmitter array and R1-R8 are represent the same for the receiver array. For example, the ultrasonic wave generated by the third element of the transmitter array (T3) takes 5.09 microseconds to be received by the seventh element of the receiver array (R7) in the parent material (Table 1). The same transmit receive data (T3R7) in the HAZ is 3.96 microseconds (Table 2) and 5.43 microseconds in the weld (Table 3). This shows that the PAUT system can detect variations of ToF in the weld, HAZ and parent material. Because the thickness of the weld strip is the same in parent material as in the HAZ and weld, there is no justification for these ToF variations which must result from residual stresses and material texture. It is always challenging to differentiate the material texture and residual stress with the ultrasonic method, which is outwith the scope of this paper.

TABLE 1: MATRIX OF 8X8 TOF IN THE PARENT MATERIAL (μS)

	R1	R2	R3	R4	R5	R6	R7	R8
T1	4.91	4.94	4.97	5.01	5.04	5.07	5.12	5.09
T2	4.98	5.01	5.01	5.04	5.05	5.11	5.14	5.16
T3	5.02	5.03	5.01	5.03	5.04	5.07	5.09	5.11
T4	5.06	5.06	5.04	5.03	5.03	5.05	5.06	5.09
T5	5.12	5.1	5.07	5.06	5.04	5.07	5.05	5.08
T6	5.22	5.18	5.14	5.11	5.1	5.09	5.07	5.1
T7	5.27	5.22	5.16	5.12	5.09	5.06	5.02	5.04
T8	5.38	5.32	5.25	5.2	5.14	5.12	5.07	5.07

TABLE 2: MATRIX OF 8X8 TOF IN THE HAZ (μS)

	R1	R2	R3	R4	R5	R6	R7	R8
T1	3.73	3.76	3.81	3.87	3.92	3.96	4.06	4.15
T2	3.76	3.78	3.82	3.86	3.9	3.95	3.99	4.07
T3	3.82	3.82	3.84	3.86	3.89	3.92	3.96	4.02
T4	3.86	3.86	3.85	3.86	3.86	3.9	3.92	3.97
T5	3.9	3.87	3.87	3.86	3.86	3.86	3.89	3.92
T6	3.96	3.92	3.91	3.9	3.87	3.87	3.87	3.9
T7	4.04	3.98	3.95	3.91	3.91	3.88	3.86	3.87
T8	4.11	4.05	4.00	3.94	3.92	3.89	3.86	3.85

TABLE 3: MATRIX OF 8X8 TOF IN THE WELD (μS)

	R1	R2	R3	R4	R5	R6	R7	R8
T1	5.19	5.18	5.31	5.39	5.72	5.04	5.47	5.52
T2	5.14	5.09	5.35	5.99	6.33	5.21	5.3	5.45
T3	5.37	5.44	5.32	5.86	5.06	5.39	5.43	5.46
T4	5.56	5.92	5.74	5.8	5.55	5.43	5.28	5.57
T5	5.59	6.35	5.16	5.48	5.3	5.33	5.4	5.28
T6	5.24	5.41	5.41	5.42	5.32	5.01	5.2	5.5
T7	5.52	5.35	5.45	5.25	5.42	5.26	5.27	5.55
T8	5.67	5.57	5.41	5.54	5.26	5.47	5.56	4.89

In this paper, the ToF variations are considered as evidence for showing the potential of using the PAUT method in the measurement of residual stress. Similar variations were also observed in the second (WAAM sample) and third (PAUT-LCR) experiments, showing the capabilities of the PAUT method for residual stress measurement in additive manufacturing and also its flexibility in generating various types of ultrasonic waves, i.e., LCR wave.

4.2 Requirements of residual stress measurement using the PAUT system

In this section, it is assumed that the material texture is the same in the parent material, HAZ and the weld in order to develop the approach and requirements of residual stress measurement using the PAUT system. It should be noted that this assumption is technically incorrect and is only used to faciliate the development of the software and hardware requirements for the residual stress measurement system. The correct method for differentiating the material texture and residual stress is the tensile test procedure, as explained in Sec. 2.1, outwith the scope of this paper. However, the same ultrasonic setup and approach are required during tensile testing and the developments of this work will be applicable in the future, to a comprehensive system that is currently in development.

It is then assumed that the parent material is a stress-free area and that its ToF matrix (Table 1) is representing T1 (see Equation 5). Therefore, if the HAZ ToF matrix is assumed to be T2, the residual stress in the HAZ can be calculated. Because *L* (acoustoelastic coefficient) was not measured in this work, it was assumed to be the same as in the data extracted by Javadi et al [12], listed in Table 4. The acoustoelastic coefficient depends on the material (which is the same in this paper and Javadi et al [12]), the component section being measured (parent material, HAZ or weld) and the frequency of the ultrasonic probe (5 MHz in this paper).

TABLE 4: ACOUSTOELASTIC COEFFICIENT RELATED TO FREQUENCY [12]

Frequency (MHz)	Parent Material	HAZ	Weld
1	2.17	1.937	2.558
2	2.102	1.839	2.452
4	2.011	1.829	2.263
5	2.132	1.96	2.462

In analysing the data, T1, T2 and σ are calculated (Equation 5) for three different approaches. Figure 9 shows the relevant geometry for calculating transmit and receive path lengths, and Equations 6-8 are used to calculate the stresses. The calculations are as follows:

1) Single Element Approach (I): In this approach (Figure 9a), it is assumed that 64 single-element transducers are used for the ToF measurement and the results of the calculations, based on Equation 6, are shown in Table 5 and 6 for the HAZ and weld, respectively:

$$\sigma_{HAZ_{Single\ Element}} = \frac{E}{L}\left(\frac{T1R1_{HAZ}-T1R1_{Parent\ Material}}{T1R1_{Parent\ Material}}\right) \quad (6)$$

2) PAUT Direct Approach (II): In the second approach (Figure 9a), only direct and straight acoustic paths (T1R1, T2R2, …, T8R8) are considered and then the average of residual stress measurement is calculated based on Equation 7:

$$\sigma_{HAZ_{PAUT-Direct}} = \frac{E}{L}\sum_{i=1}^{n}\left(\frac{TiRi_{HAZ}-TiRi_{Parent\ Material}}{TiRi_{Parent\ Material}}\right)/n \quad (7)$$

3) PAUT-FMC Approach (III): In this approach (Figure 9b), all possibilities for the acoustic path (T1R3, T6R1, T8R8, etc.) are considered. This is similar to the Full Matrix Capturing (FMC) approach which is widely used in the PAUT method. Therefore, the average of 8x8 residual stress is calculated based on Equation 8:

$$\sigma_{HAZ_{PAUT-FM}} = \frac{E}{L}\sum_{i=1}^{n}\ \sum_{j=1}^{n}\left(\frac{TiRj_{HAZ}-TiRj_{Parent\ Material}}{TiRj_{Parent\ Material}}\right)/n^2 \quad (8)$$

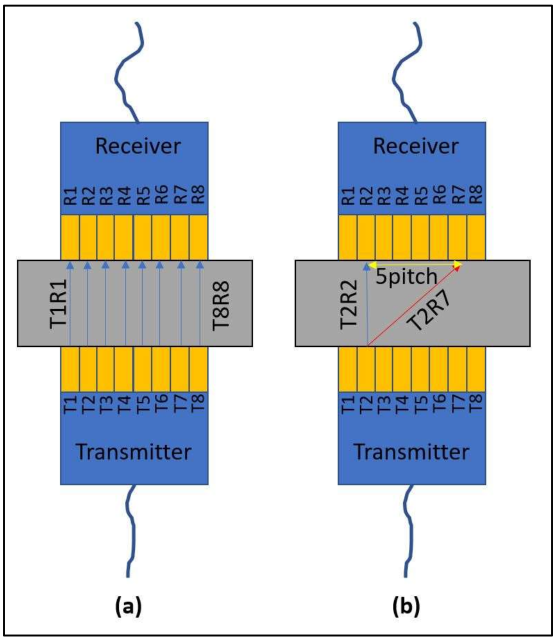

FIGURE 9: DATA ANALYSIS FOR THE PAUT RESIDUAL STRESS MEASUREMENT USING APPROACH I&II (A) AND APPROACH III (B)

TABLE 5: ESTIMATED RESIDUAL STRESS IN HAZ USING APPROACH I (DATA ARE IN MPA)

	R1	R2	R3	R4	R5	R6	R7	R8
T1	-21	-21	-21	-20	-20	-19	-18	-16
T2	-22	-22	-21	-21	-20	-20	-20	-19
T3	-21	-21	-21	-21	-20	-20	-20	-19
T4	-21	-21	-21	-21	-21	-20	-20	-19
T5	-21	-21	-21	-21	-21	-21	-20	-20
T6	-21	-22	-21	-21	-21	-21	-21	-21
T7	-21	-21	-21	-21	-21	-21	-20	-21
T8	-21	-21	-21	-21	-21	-21	-21	-21

TABLE 6: ESTIMATED RESIDUAL STRESS IN WELD USING APPROACH I (DATA ARE IN MPA)

	R1	R2	R3	R4	R5	R6	R7	R8
T1	5	4	6	7	12	-1	6	7
T2	3	2	6	17	22	2	3	5
T3	6	7	5	15	0	6	6	6
T4	9	15	12	14	9	7	4	8
T5	8	22	2	7	5	5	6	3
T6	0	4	5	5	4	-1	2	7
T7	4	2	5	2	6	3	4	9
T8	5	4	3	6	2	6	9	-3

From Tables 5 and 6, it can be seen there is a variation in the estimated residual stress depending on the different combinations of the transmitter-receiver element number. For example, if T1R1 is chosen, the HAZ residual stress is -21 MPa while this is -16 MPa in the case of choosing T1R8. The variations are larger in the weld where the residual stress is reported from -3 MPa (T8R8) to 22 MPa (T5R2). It should be noted that this variation is undesirable as the residual stress cannot change as sharply in the small area covered by the arrays. This is one of the main disadvantages of using the single element transducer method, where only one measurement is carried out. Because the PAUT probes are used in this work, it is assumed that 64 different possibilities of probes positions are available. Taking the same number of measurements with single element transducers is impractical and this makes it difficult to determine the same potential measurement error when using the single element system. This error can be reduced if the ultrasonic array is used and then the data is averaged (Approach II and III) as shown in Table 7. Given the higher calculations demand for the FMC (approach III), a MATLAB script was developed and linked to the LabView interface of the phased array controller. The requirements for a residual stress measurement system using the PAUT method (based on approach III) includes the PAUT probes (small footprint), phased array controller (coupled with two arrays as transmitter and receiver) and a Matlab script linked with the LabView interface.

TABLE 7: RESULTS OF RESIDUAL STRESS MEASUREMENTS USING THREE APPROACHES (I, II AND III)

	HAZ	Weld
Approach I	-16 MPa to -21 MPa	-3 MPa to 22 MPa
Approach II	-21 MPa	-4 MPa
Approach III	-21 MPa	-6 MPa

Although the interpretation of the residual stress data is outwith the scope of this paper (as the material texture effects are excluded), it is obvious that increasing the number of ToF measurements can enhance the accuracy of the residual stress evaluation. It is worth mentioning that the stress variations and measurement uncertainty in the weld and HAZ were expected, as reported by Javadi et al [12], in the ultrasonic method. Therefore, it is recommended that the single element transducers be replaced by the PAUT system for residual stress measurement of welds and WAAM components in future. However, this paper only covers the hardware and software requirements of such a system and a comprehensive study of the residual stress using the PAUT system is required. The final development will have to include a smart system for differentiation of the material texture from the residual stress. Furthermore, it will need to include a comprehensive verification procedure using multiple stress measurement techniques.

5. CONCLUSION

In this paper, the feasibility of using a PAUT system for residual stress measurement in welding and WAAM was investigated. Based on the results, it can be concluded that:

1) The PAUT system can detect the ToF variations in the parent material, HAZ and weld. If the effect of material texture on the ultrasonic wave is differentiated from the effect of residual stress, the system can be used for residual stress measurement.
2) The same ToF variations were observed in the WAAM sample, showing the potential of the PAUT method for residual stress measurement in additively manufactured components.
3) The PAUT-LCR system was developed and it can successfully detect the ToF variations in a machined weld sample with the cap removed.
4) Three residual stress measurement approaches (Single Element, PAUT-Direct and PAUT-FMC) were studied. The single element approach can result in measurement error, especially in the weld, which can be reduced by using the PAUT-FMC approach.
5) The requirements for a residual stress measurement system that works based on the PAUT-FMC approach, includes small footprint arrays, phased array controller and Matlab script linked with the LabView interface.

It is recommended that the PAUT setup developed in this work is used in a comprehensive system of residual stress measurement which includes tensile testing, to differentiate material texture from residual stress. The results should be validated through a comprehensive verification procedure using the standard hole drilling method and other residual stress measurement techniques.

REFERENCES

[1] Y. Javadi, N.E. Sweeney, E. Mohseni, C.N. MacLeod, D. Lines, M. Vasilev, Z. Qiu, C. Mineo, S.G. Pierce, A. Gachagan, Investigating the effect of residual stress on hydrogen cracking in multi-pass robotic welding through process compatible non-destructive testing, Journal of Manufacturing Processes (2020).

[2] F. Martina, M.J. Roy, B.A. Szost, S. Terzi, P.A. Colegrove, S.W. Williams, P.J. Withers, J. Meyer, M. Hofmann, Residual stress of as-deposited and rolled wire plus arc additive manufacturing Ti-6Al-4V components, Materials Science and Technology 32 (2016) 1439-1448.

[3] L. Pérez Caro, E.-L. Odenberger, M. Schill, F. Niklasson, P. Åkerfeldt, M. Oldenburg, Springback prediction and validation in hot forming of a double-curved component in alloy 718, International Journal of Material Forming 6 (2021).

[4] J.C. Outeiro, A.M. Dias, J.L. Lebrun, V.P. Astakhov, MACHINING RESIDUAL STRESSES IN AISI 316L STEEL AND THEIR CORRELATION WITH THE CUTTING PARAMETERS, Machining Science and Technology 6 (2002) 251-270.

[5] Y. Javadi, J.N. Walsh, A. Elrefaey, M.J. Roy, J.A. Francis, Measurement of residual stresses induced by sequential weld buttering and cladding operations involving a 2.25Cr-1Mo substrate material, International Journal of Pressure Vessels and Piping 154 (2017) 58-74.

[6] Y. Javadi, M.C. Smith, K. Abburi Venkata, N. Naveed, A.N. Forsey, J.A. Francis, R.A. Ainsworth, C.E. Truman, D.J. Smith, F. Hosseinzadeh, S. Gungor, P.J. Bouchard, H.C. Dey, A.K. Bhaduri, S. Mahadevan, Residual stress measurement round robin on an electron beam welded joint between austenitic stainless steel 316L(N) and ferritic steel P91, International Journal of Pressure Vessels and Piping 154 (2017) 41-57.

[7] M.M. Shokrieh, A.R.G. K, Simulation of Central Hole Drilling Process for Measurement of Residual Stresses in Isotropic, Orthotropic, and Laminated Composite Plates, Journal of Composite Materials 41 (2006) 435-452.

[8] Gary S. Schajer, P.S. Whitehead, Hole-Drilling Method for Measuring Residual Stresses, Morgan & Claypool Publishers2018.

[9] Y. Javadi, E. Mohseni, C.N. MacLeod, D. Lines, M. Vasilev, C. Mineo, S.G. Pierce, A. Gachagan, High-temperature in-process inspection followed by 96-h robotic inspection of intentionally manufactured hydrogen crack in multi-pass robotic welding, International Journal of Pressure Vessels and Piping 189 (2021) 104288.

[10] J. Hönnige, C.E. Seow, S. Ganguly, X. Xu, S. Cabeza, H. Coules, S. Williams, Study of residual stress and microstructural evolution in as-deposited and inter-pass rolled wire plus arc additively manufactured Inconel 718 alloy after ageing treatment, Materials Science and Engineering: A 801 (2021) 140368.

[11] J.A. Francis, H.K.D.H. Bhadeshia, P.J. Withers, Welding residual stresses in ferritic power plant steels, Materials Science and Technology 23 (2007) 1009-1020.

[12] Y. Javadi, M. Akhlaghi, M.A. Najafabadi, Using finite element and ultrasonic method to evaluate welding longitudinal residual stress through the thickness in austenitic stainless steel plates, Materials & Design 45 (2013) 628-642.

[13] A. International, ASTM E837-13a Standard Test Method for Determining Residual Stresses by the Hole-Drilling Strain-Gage Method, West Conshohocken, PA, 2013.

[14] M.B. Prime, M.R. Hill, A.T. DeWald, R.J. Sebring, V.R. Dave, M.J. Cola, Residual stress mapping in welds using the contour method, Trends in Welding Research, Proceedings (2003) 891-896.

[15] N.S. Rossini, M. Dassisti, K.Y. Benyounis, A.G. Olabi, Methods of measuring residual stresses in components, Materials & Design 35 (2012) 572-588.

[16] M.D. Olson, M.R. Hill, B. Clausen, M. Steinzig, T.M. Holden, Residual Stress Measurements in Dissimilar Weld Metal, Experimental Mechanics 55 (2015) 1093-1103.

[17] P.B. Nagy, Opportunities and Challenges for Nondestructive Residual Stress Assessment, AIP Conference Proceedings 820 (2006) 22-40.

[18] D.M. Egle, D.E. Bray, Measurement of acoustoelastic and third-order elastic constants for rail steel, The Journal of the Acoustical Society of America 60 (1976) 741-744.

[19] Y. Javadi, M. Ashoori, Sub-surface stress measurement of cross welds in a dissimilar welded pressure vessel, Materials & Design 85 (2015) 82-90.

[20] Y. Javadi, M.A. Najafabadi, M. Akhlaghi, Comparison between Contact and Immersion Method in Ultrasonic Stress Measurement of Welded Stainless Steel Plates, Journal of Testing and Evaluation 41 (2013) 788-797.

[21] Y. Javadi, M. Akhlaghi, M.A. Najafabadi, Nondestructive Evaluation of Welding Residual Stresses in Austenitic Stainless Steel Plates, Research in Nondestructive Evaluation 25 (2014) 30-43.

[22] Y. Javadi, M. Hasani, S. Sadeghi, Investigation of Clamping Effect on the Welding Sub-surface Residual Stress and Deformation by Using the Ultrasonic Stress Measurement and Finite Element Method, Journal of Nondestructive Evaluation 34 (2015).

[23] A.H. Yaghi, T.H. Hyde, A.A. Becker, W. Sun, Finite element simulation of residual stresses induced by the dissimilar welding of a P92 steel pipe with weld metal IN625, International Journal of Pressure Vessels and Piping 111 (2013) 173-186.

[24] D.I.A.W. Lines, J; Hottenroth, J, Real-time full matrix capture + total focusing and other novel imaging options using general purpose PC-based array instrumentation, Insight 5 (2012) 86-90.